Biosensors and Bioelectronics 26 (2011) 3914–3919

Contents lists available at ScienceDirect

Biosensors and Bioelectronics

journal homepage: www.elsevier.com/locate/bios

Multi-panel drugs detection in human serum for personalized therapy

Sandro Carrara [a,*], Andrea Cavallini [a], Victor Erokhin [b], Giovanni De Micheli [a]

[a] Integrated Systems Laboratory – EPFL – École Polytechnique Fédérale de Lausanne, Switzerland
[b] CNR-IPCF (Rome) and Department of Physics – Parma University – Parma, Italy

ARTICLE INFO

Article history:
Received 13 December 2010
Received in revised form 8 March 2011
Accepted 9 March 2011
Available online 17 March 2011

Keywords:
Carbon nanotubes
Cytochromes P450
Drugs detection
Multi-drug detection
Personalized therapy

ABSTRACT

This work focuses on P450 biosensors based on *multiwalled carbon nanotubes* (MWCNT) and different cytochrome isoforms: 3A4, 2B4, 2C9. The proposed biosensors exhibit enhanced sensitivities and decreased detection limits thanks to carbon nanotubes. The MWCNT structuring improves the sensitivity from 5.1 to 20.5 nA/mM mm^2 in case of CYP2B4-mediated Benzphetamine detection, from 0.26 to 0.63 nA/μM mm^2 in case of CYP3A4-mediated Cyclophosphamide detection, and from 0.11 to 0.25 nA/μM mm^2 in case of CYP2C9-mediated Naproxen detection. By using MWCNT, the limit of detection was enhanced from 59 to 12 μM in case of Cyclophosphamide and from to 187 to 82 μM in case of Naproxen. This makes possible the drug detection in human serum within the pharmacological range. In the paper, a new mathematical model is also proposed to succeed in discriminating different drug contributions in a mixture containing both Cyclophosphamide and Dextromethorphan or combining Naproxen and Flurbiprofen. Data analysis shows variations in reduction peaks that are dependent on the drug ratio, and that are consistent with competitive kinetics of substrates. This new approach enables multiple drug detection and opens the way to possible applications in personalized therapy.

1. Introduction

The development of new technologies in personalized therapy is required to increase the fraction of patients that can benefit of pharmacological treatments. For many of the major pathologies, the average rate of efficacy of drug therapies ranges from 20% to 60% (Aspinall and Hamermesh, 2007). Moreover, approximately 7% of hospitalized patients experience serious adverse drug reactions (Lazarou et al., 1998). For this reason, drug therapy needs personalization to the individual patient (Daly, 2007; Turner et al., 2007). One of the reasons for this variability is genetic polymorphisms. For example, variations in cytochrome P450 2D6 (Frank et al., 2007), an enzyme that accounts for the metabolism of 19% of known drugs (Kashuba and Bertino, 2003), causes overdosing in "poor metabolizers" and underdosing in "ultrafast metabolizers". This classification affects the bioavailability of the active compounds after a single administration, as demonstrated for Nortriptyline (Lin, 2007).

At present, the only strategy for personalizing the drug therapies is to check the genetic predisposition of patients. The AmpliChip CYP450 (De Leon et al., 2006) is a genetic test based on microarray technology commercialized by Roche. It screens genetic mutations on CYP2D6 and CYP2C19, yielding a classification of patients in poor, intermediate, extensive, and ultra-rapid metabolizers.

Although this technology represents a great improvement with respect to the traditional approach, the sole knowledge of genotype is not sufficient to achieve the maximum accuracy in drug administration, since human metabolism may vary in short time periods and it is related to patients' nutrition, history, attitudes, and environmental conditions.

Drug metabolism should be monitored on a daily basis to optimize any ongoing drug therapy. However, therapeutic drug monitoring, i.e., quantification of drug concentrations after administration to see whether the desired concentration range has been reached, is available only in large clinical chemistry labs, with bulky and expensive equipment. A reliable low-cost technology to monitor multiple drug compounds in patients for personalized treatments at point-of-care can be developed using cytochromes P450 as probe proteins. Biosensors based on individual P450 proteins have already been proposed (Iwuoha et al., 2007; Joseph et al., 2003; Liu et al., 2008); unfortunately, the detection sensitivity achieved is often too far from the drug therapeutic ranges for real applications in human serum. Recently it has been shown how a major improvement in P450 sensitivity can be obtained from electrode nanostructuring, using materials like zirconium dioxide (Peng et al., 2008), gold nano-particles (Shumyantseva et al., 2005), or carbon nanotubes (Carrara et al., 2008).

In this paper, we propose a multi-panel approach for developing biosensors based on multiwalled carbon nanotubes (MWCNT) and three different cytochrome P450 isoforms: the 3A4, 2B4, 2C9. The paper presents results in detecting different drugs: Benzphetamine, a compound used in anti-obesity treatments; Cyclophosphamide,

* Corresponding author. Tel.: +41 21 693 0915; fax: +41 21 693 0909.
E-mail address: sandro.carrara@epfl.ch (S. Carrara).

0956-5663/$ – see front matter © 2011 Elsevier B.V. All rights reserved.
doi:10.1016/j.bios.2011.03.009

an anti-cancer agent; Dextromethorphan, a drug commonly used as cough suppressant; Naproxen and Flurbiprofen, two widespread anti inflammatory compounds. The usage of MWCNT improves the sensor sensitivity, reaching the range to discriminate the presence of drugs in human serum and within the pharmacological range. The measurement at different electrochemical potentials improves the specificity and supports the possibility of multiple drug detection. In particular, different drug contributions in multiple detection are determined by fitting the cyclic voltammograms with Gaussian decomposition and accounting for cross-interfering form different drug compounds on the same CYP protein. A new model is proposed for the right estimation of each Gaussian amplitude. The results demonstrate that the reached sensitivity and specificity are suitable for applications in personalized therapy and open the possibility to the realization of sensors for point-of-care monitoring by patient's even at home.

2. Materials and methods

2.1. Reagents

Carbon paste screen-printed electrodes (model DRP-110) were purchased from Dropsens. Cytochrome P450 2B4 was isolated and purified from the microsomal fraction of rabbit (Shumyantseva et al., 2007). Cytochrome 2B4 and Benzphetamine substrates were received from the Institute of Biomedical Chemistry of the Russian Academy of Biomedical Science. Cytochrome P450 3A4 and 2C9 microsomes were purchased from Sigma–Aldrich, and used without further purification. Cyclophosphamide (CP) and Dextromethorphan (DX) was purchased from Sigma and diluted in PBS 100 mM pH 7.4 to the working concentrations. Naproxen (NP) and Flurbiprofen (FB) was purchased from Sigma and diluted in ethanol to the working concentrations. Multi walled carbon nanotubes (MWCNT – diameter 10 nm, length 1–2 μm, COOH content 5%) were purchased in powder (95% purity) from DropSens (Spain), diluted in chloroform to the concentration of 1 mg/ml, and then sonicated for 20 min in order to break macro-aggregates. Human serum was purchased from Lonza and used without any dilution.

2.2. Electrode preparation

The screen-printed electrodes were purchased from DropSens, Spain. They were fabricated with of a graphite or a gold working electrode, a graphite or a platinum counter electrode and a silver reference electrode. The working electrode area is 12.56 mm^2 while the total area of the cell is 22 mm^2. CNT nano-structuring was obtained by gradually dropping 30 μl of CNT solution onto the working electrode and waiting until complete evaporation of the chloroform. Electrode functionalization was obtained by drop casting P450 solutions onto the working electrode and incubation at 4 °C overnight. The excess of cytochrome was then removed by washing with milliQ water.

2.3. SEM measurement

Morphological analysis of the structured and functionalized electrodes was done using a *Scanning Electron Microscope* (SEM). A Zeiss SUPRA 40 SEM instrument was used to acquire images for bare, CNT-structured and P450-functionalized electrodes. Images were acquired in the 5–20 kV range.

2.4. Size analysis on SEM images

The program ImageJ (Abramoff et al., 2004) was used to calculate the average diameters and the standard deviations for the fibers recognized in the SEM images. To analyze the obtained results, Monte Carlo method (Hammersley and Handscomb, 1975) was used to simulate proteins deposition on carbon nanotubes. The P450 proteins are globular proteins, and their 3-D structure may be included in a sphere of 8 nm (Locuson and Tracy, 2006), as confirmed by direct AFM imaging on P450 samples (Kiselyova et al., 1999). Although the different isoforms of the P450 cytochrome exhibit similar sizes, we need to take into account a more precise estimation for the protein diameter. Therefore, the Crystal 3-D structure of the human microsomal P450 3A4 presents in the protein RCSB Protein Data Bank (Yano et al., 2004) was used as model to precisely estimate the average diameter of the protein in a random orientation. Different carbon nanotube diameters were randomly selected among those measured in SEM images of non-functionalized samples. Then, 10,000 depositions onto carbon nanotubes of proteins in random orientation where simulated in order to estimate the final average diameter reached by the fiber.

2.5. Electrochemical measurement

The electrochemical response of the biosensor was investigated with cyclic voltammetry under aerobic conditions. Voltammograms were acquired using a Versastat 3 potentiostat (Princeton Applied Technologies). The electrode was covered with 100 μl of PBS 10× at pH 7.4, or serum. Drug samples were added in drops of 1 μl. The cyclic voltammograms were acquired with potential sweeps between −600 and +300 mV vs. Ag/AgCl at a scan rate of 20 mV/s. Peak current values were then extracted according to the procedure reported in (Carrara et al., 2009).

3. Results and discussion

3.1. AFM imaging

Fig. 1A shows bundles of MWCNT cast onto carbon paste screen-printed electrodes. The nanotubes are randomly organized in a net that greatly increases the surface available for the protein adsorption. Fig. 1B shows that the apparent thickness of the carbon nanotubes increases after the probe immobilization. A direct comparison of the apparent fiber sizes in SEM images is used to show that no more than one protein layer surrounds the single carbon nanotube. Indeed, size analysis performed on different SEM images shows that this increase goes from 11.14 ± 2.59 nm, in case non-functionalized MWCNT, to 19.51 ± 5.72 nm, in case of the MWCNT functionalized with microsomes containing the protein P450 3A4. Simulated depositions done by using the Monte Carlo method return a final diameter for a single layer of P450 3A4 proteins surrounding the carbon nanotube equal to 21.71 ± 2.78 nm. The average diameter obtained from SEM measurements does not statistically differ from that obtained from Monte Carlo simulations. Therefore, we can conclude that a single layer of probe proteins is surrounding each single nanotube fiber. Taking into account that the 3A4 proteins are dispersed onto the carbon nanotubes when they are embedded in microsomes, a fiber diameter that is much smaller than that of a typical microsome means that the carbon nanotube breaks the microsome. Thus, the P450 probes are in direct contact with the tube surface. Consequently, even with samples of P450 probes embedded in microsomes, carbon nanotubes assure a direct electron-transfer to the P450 proteins, as obtained in the past with other P450 isoforms immobilized after protein purification (Carrara et al., 2008). On the other hands, the average diameter is larger in the simulations than that measured in the SEM images. Moreover, the measure of its standard deviation in SEM images is larger than that theoretically estimated. This means that other components of the microsome (pieces of membrane, P450 reduc-

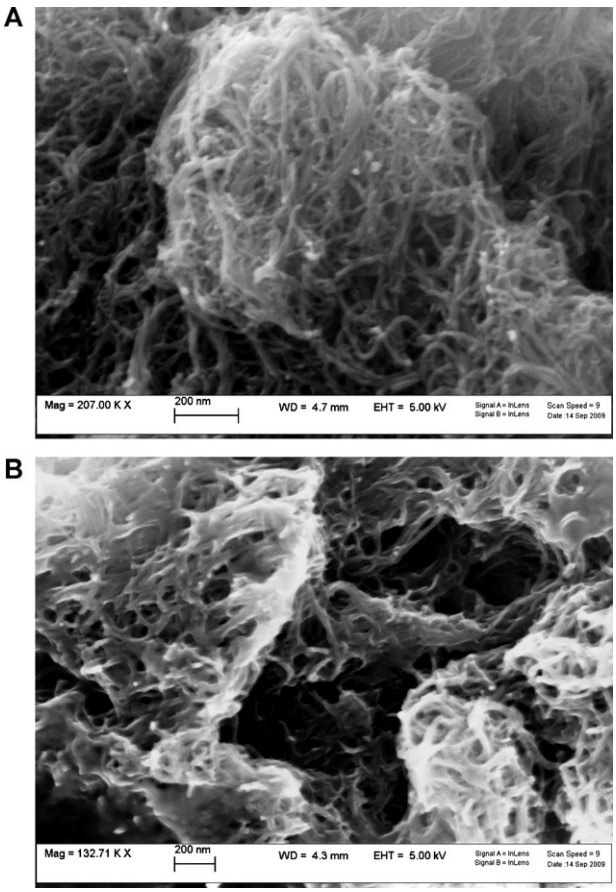

Fig. 1. SEM images showing screen-printed carbon-paste electrodes as structured by using multi-walled carbon nanotubes (A) and after immobilization with P450 3A4 proteins (B).

tases, etc.) may also contribute to the bio-layer coating the carbon nanotube.

3.2. Improved detection limit

We registered an improved sensitivity during drug detection using cytochromes adsorbed onto carbon nanotubes. Fig. 2 shows two calibration curves estimated from Faradic current peaks measured with cyclic voltammetry. These calibrations show current increase in presence of increasing drug amounts. The figure clearly shows that the detection limit obtained in the case of the P450 immobilized onto bare screen-printed electrodes is close to 75 μM. This is not enough because the range of concentration found in patients' serum (the so called "therapeutic range") for the Cyclophospamide is from 2.6 μM to 76.6 μM (Juma et al., 1979). On the other hand, Fig. 2 shows that MWCNT are definitely required to fit the required concentrations window.

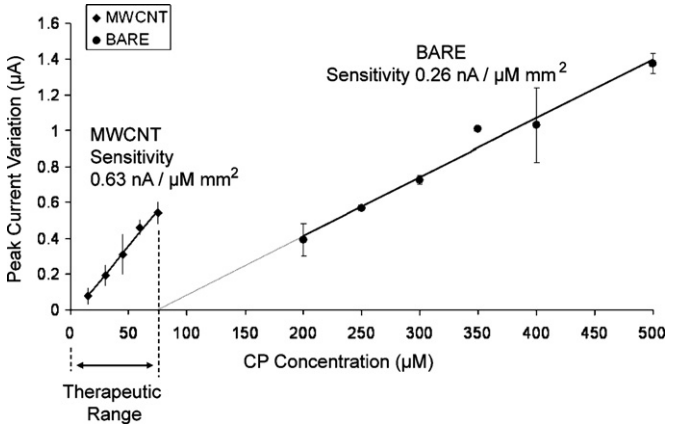

Fig. 2. Calibration curves in detection of Cyclophosphamide (CP) from peak currents as registered in cyclic voltammograms acquired with P450 3A4 immobilized onto screen-printed electrodes with or without multi walled carbon nanotubes. The voltammograms were acquired with the drug dissolved in PBS and at the scan velocity of 20 mV/s.

The enhancement provided by carbon nanotubes is crucial to realize biosensors for drug monitoring. One of the biggest obstacles to overcome in drug detection is the capability to sense compounds in serum with concentrations ranging typically in the order of μM or nM. Most of P450-based biosensors proposed in literature demonstrate detection windows in the mM scale. For example, P450 detection of Verapamil is shown for concentrations of 0.5–3 mM (Joseph et al., 2003), which is orders of magnitude higher then its pharmacological range, typically below 55 nM (Eichelbaum et al., 1981). Similarly, detection of Benzphetamine is listed in Table 1 of Supplementary Files (published online) in the range 0.5–4 mM, which is not suitable for real applications since the amphetamine level in human blood is below 74 nM (Schepers et al., 2003).

In order to compare our detection limits reached by using carbon nanotubes with concentration levels in human blood, more precisely estimations were done by considering the IUPAC definition (Mc Naught and Wilkinson, 1997):

$$\text{L.O.D.} = \frac{k\delta i}{S} \quad (1)$$

where L.O.D. is the limit of detection, δi is the standard deviation of the blank measures, S is the detector sensitivity, and k is a parameter accounting for the confidence level ($k = 1$, 2, or 3 corresponds to 68.2%, 95.4%, or 99.6% of statistical confidence). The background has been subtracted before the computation of the L.O.D. with Eq. (1) because it is only due to double-layering phenomenon related to carbon nanotubes (Carrara et al., 2005) and it is not related to the drugs detection as performed by the P450 cytochromes.

In the case of the Cyclophospamide, the detection limit from definition (1) goes down from 59 μM to 12 μM, once the protein is immobilized onto MWCNT. The improved L.O.D fits quite well with a concentration level in patients below 76.6 μM (Juma et al., 1979). Similarly, we got improvement from 187 to 82 μM in the case of Naproxen detected with the protein P450 2C9 immobilized into MWCNT. Even in this case, the improved L.O.D. fits better with the concentration level in patients, which range from 21 to 515 μM (Korzekwa et al., 1998).

Fig. 3 shows that we also obtained similar results in the detection of Cyclophosphamide in human serum. Using the P450 3A4 on MWCNT, the detection limit reached in serum was at 33 μM, according to definition (1). This detection limit fits quite well with windows of concentration of Cyclophosphamide found in patients' plasma for some applications, which varies between 3.8 and 157 μM (Struck et al., 1987). Thus, our result shows that drug detection is also possible in human serum when the CYP proteins are immobilized onto carbon nanotubes, because they ensure higher sensitivity and lead to lower detection limits.

Table 1 of the Supplementary Files (published on line) summarizes the sensitivity enhancements we obtained after immobilizing different P450 proteins on MWCNT. The sensitivity in case of CYP2B4-mediated detection of benzphetamine increases from 5.1 nA/mM mm^2 to 20.5 nA/mM mm^2. The sensitivity for CYP3A4-mediated detection of Cyclophosphamide increases from 0.26 to 0.63 nA/mM mm^2, and that for Naproxen from 0.11 to 0.25 nA/mM mm^2. Similar sensitivity enhancement has been recently obtained using MWCNT for hydrogen peroxide based

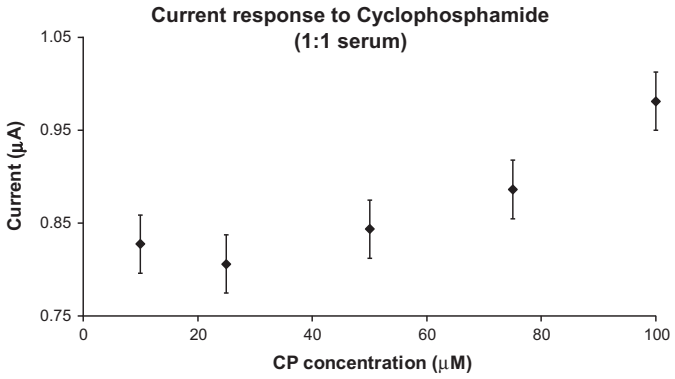

Fig. 3. Peak currents as estimated in cyclic voltammograms acquired with P450 3A4 immobilized onto multi walled carbon nanotubes during the detection of Cyclophosphamide (CP). The voltammograms were acquired with the drug dissolved in human serum and at the scan velocity of 20 mV/s.

detection. In that case, a sensitivity gain up to seven times has been registered (Boero et al., 2009).

3.3. A new approach to improve specificity

Another crucial aspect in the P450 biosensor development is its specificity. Multi-component Faradic currents are measured when a drug cocktail is present in the blood. Every cytochrome isoform is capable to metabolize a broad range of compounds. For example, the CYP2C9 may sense Torsemide, as well as Diclofenac, Tolbutamide, S-Warfarin, and Sulfaphenazole (Johnson et al., 2005). Nevertheless, it is also well known that, often, different Faradic currents in cyclic voltammograms are shifted towards different potentials. On CYP2C9, Torsemide presents a current peak at the potential of −19 mV, while Diclofenac exhibits a current maximum at −41 mV (Johnson et al., 2005). The Figure reported in the Supplementary Files (published online) confirms this feature of the *drug electrochemical signature*: the plot shows that Cyclophosphamide (CP) is detected at −296 mV, while Dextromethorphan (DX) at −392 mV, confirming that multiple drugs can be simultaneously detected using a single cytochrome isoform.

In the case of multi-detection by means of single P450 protein, we need to take into account cross-correlations between different compounds. Measures on the same amount of CP drug (400 μM) repeated in presence of different amount of the DX (ranging from 0 to 400 μM) result in different registered currents for the Faradic peak corresponding to CP in the cyclic voltammogram, as clearly shown by Fig. 4. In particular, we observed smaller currents corresponding to the same amount of CP for increasing amounts of DX. This is coherent with the phenomenon of inhibition already observed in some cases of P450 enzymatic activity (Tracy, 2003). Due to this phenomenon, the Faradic current related to detection of the single drug component is not only related to the amount of that drug. It is also affected by the concentrations of the other interfering drugs present into the sample.

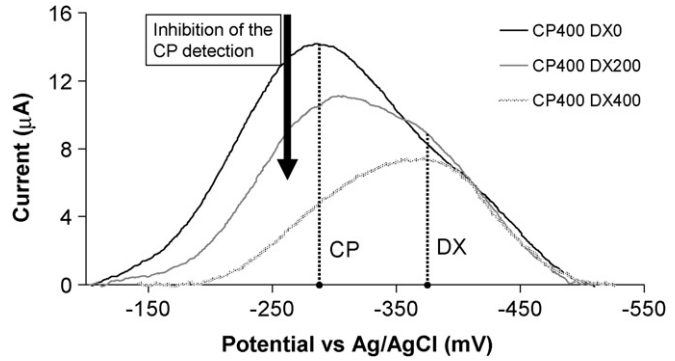

Fig. 4. Cyclic voltammograms acquired with P450 3A4 immobilized onto multi walled carbon nanotubes during the simultaneous detection of Cyclophosphamide (CP) and Dextromethorphan (DX), at different concentration of DX. The voltammograms were acquired with the drugs dissolved in PBS and at the scan velocity of 20 mV/s.

A general approach for a correct estimation of the drug amounts in the sample is still possible by considering that the Faradic current can be decomposed in Gaussian components:

$$i(V) = \sum_{\forall k} \Gamma_k C_k \left\{ \prod_{\forall j \neq k} A_k\left(C_j\right) \right\} e^{-\frac{\left(V - V_k\right)^2}{\sigma_k^2}} \tag{2}$$

where the term Γ_k is defined as:

$$\Gamma_k = 0.4463 \left(\frac{n^3 F^3 \nu D_k}{RT} \right)^{1/2} A \tag{3}$$

So, the final current will be the sum of all the Gaussian contributions of each single drug. Every single contribution will vary in a dynamic manner, according to the concentration of all the specimen in solution. Coherently with the Randles-Sevcik equation (Bard and Faulkner, 2001), Eqs. (2) and (3) account for the concentration and diffusion coefficients of each single drug (C_k and D_k). V_k are the positions of each component, σ_k are the component widths, and the $A_k(C_j)$ are the component amplitudes that also depend on the concentration of all the other interfering drugs (C_j). The other parameters in the Eqs. (2) and (3) are the usual ones of the Randles-Sevcik equation: n is the number of electrons involved in the redox, F is the faraday constant, ν is the scan-rate of the voltammetry, A is the electrochemical active area, R is the gas constant, T is the temperature.

For the amplitude of these Faradic components, we need now to take into account the kinetics of the P450/drug interactions for the interfering compounds. For usual metabolic kinetics, the enzymatic-inhibition of the detection on the drug compound k from the interfering compound j will be mediated by the Michaelis–Menten kinetics as:

$$A_k\left(C_j\right) = A_{k0}\left(1 - \varepsilon_j w_j\right) \tag{4}$$

The w_j is the reaction rate of the interfering drugs that follows the Michaelis–Menten equation (Naka and Sakamoto, 1992):

$$w_j = \frac{V_{\max} C_j}{K_M + C_j} \tag{5}$$

where V_{max} and K_M are the usual kinetic parameters for the maximal velocity and for the concentration of substrate at which half-maximal velocity is achieved (Naka and Sakamoto, 1992). The parameter A_{k0} is the amplitude of the k-Gaussian, and C_j is the concentrations of the interfering drug. The new parameter ε_j takes into account the interference strength, and it may have values in the range from zero to unity.

Analogously, in the case of the simultaneous detection of the Naproxen (NP) and the Flurbiprofen (FP), we registered increasing Faradic currents corresponding to the same amount of FL (200 μM) in the presence of increasing amounts of NP (from 0 to 500 μM), as clearly shown by Fig. 5. Even in this case, the observed increasing in current is coherent with the phenomenon of enzymatic-activation observed in some cases of P450 enzymatic activity (Tracy, 2003). In this case, the amplitude of the Faradic components becomes:

$$A_k\left(C_j\right) = A_{k0}\left(1 + \varepsilon_j w_j\right) \tag{6}$$

Eq. (6) differs from Eq. (4) only with the sign in front of the Michaelis–Menten term. The Michaelis–Menten Eq. (5) is used to enhance the Faradic current in Eq. (6), while it is used to depress

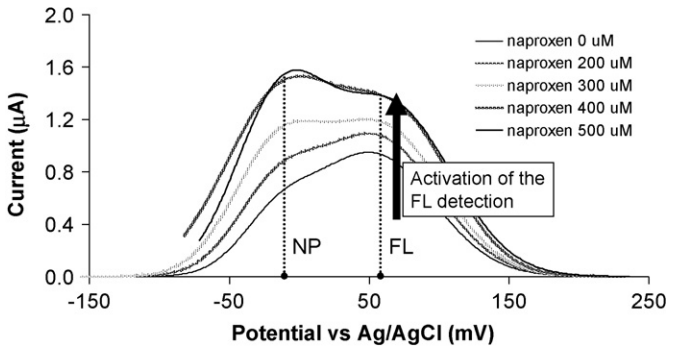

Fig. 5. Cyclic voltammograms acquired with P450 2C9 immobilized onto multi walled carbon nanotubes during the simultaneous detection of Naproxen (NP) and Flurbiprofen (FL), at different concentration of NP. The voltammograms were acquired with the drugs dissolved in PBS and at the scan velocity of 20 mV/s.

the Faradic current in Eq. (4). So, the Eq. (6) may be used to analyze the data contained in Fig. 5, where the Naproxen (NP) interferes by enhancing the current related to the Flurbiprofen (FL) detection. Eq. (4) may be instead used to analyze the data contained in Fig. 4, where the Dextromethorphan (DX) interferes by depressing the current related to the Cyclophosphamide (CP) detection.

More in general, different drugs may follow atypical kinetics instead Michaelis–Menten one. On the cytochromes 2C9, Flurbiprofen follows Michaelis–Menten kinetics, while Naproxen fits better with the biphasic model, Dapson with sigmoidal model, and Piroxicam with substrate partial-inhibition (Tracy, 2003). So, we need to generalize the Eqs. (4) and (6) in order to account for other kinetics. In case of the enzymatic-inhibition, we can write:

$$A_k\left(C_j\right) = A_{k0}\left\{1 - \varepsilon_j \Phi\left(x_1, x_2, x_3, \ldots x_n\right)\right\} \quad (7)$$

where Φ is the model-function that generalizes for different kinetics involved by the interfering drugs. This function Φ depends on different parameters:

$$\left(x_1, x_2, x_3, \ldots x_n\right) = \left(C_j, V_{\max,j}, K_{M,j}, CLint_{1,j}, CLint_{2,j}, \ldots\right) \quad (8)$$

which are the drug concentration, maximal velocity, concentration for achieving half-maximal velocity, but also depends by parameters like $CLint_1$ and $CLint_2$, which are the intrinsic clearances usually considered in atypical pharmacokinetics (Tracy, 2003). Of course, other parameters may be introduced in the Eq. (8), depending on the kind of atypical kinetics is followed by the interfering compound. In the case of enzymatic-activation, the Eq. (7) becomes:

$$A_k\left(C_j\right) = A_{k0}\left\{1 + \varepsilon_j \Phi\left(x_1, x_2, x_3, \ldots x_n\right)\right\} \quad (9)$$

Eqs. (2), (3), (7) and (9) show that the right identification and quantification of each single drug in the electrochemical signature as registered by the cyclic voltammograms may be not so trivial, while Eqs. (4)–(6) give the simplified model in case of compounds following the Michaelis–Menten kinetics. In any case, the development of potentiostats, on either printed circuit board and on-chip, enabling the acquisition of full voltammograms as well as the automatic data analysis with Gaussian decomposition is definitely required to succeed in applications for personalized therapy in monitoring the patients' metabolism on drugs.

4. Conclusions

In this work, we developed high-sensitive biosensors supporting multi-panel detection to provide information on multi-drug metabolism in human serum. Different P450 isoforms were immobilized on multi-walled carbon nanotubes in order to improve sensor sensitivity. Drug detection and relative performance were shown for Benzphetamine, Cyclophosphamide, Dextromethorphan, Naproxen, and Flurbiprofen.

The sensor proved, in case of Cyclophosphamide and Naproxen, to be able to measure drug amounts comparable to the ones found in patients during standard therapeutic regime. Moreover, we have been able to perform Cyclophopshamide measurements into its therapeutic range in undiluted human serum. These results prove to be suitable for measurements in patients and, consequently, the proposed approach can be used in personalized therapies.

The proposed technology also enables the identification of different drugs, as directly demonstrated for the simultaneous detection of Cyclophosphamide and Dextromethorphan with CYP3A4 and the simultaneous detection of Naproxen and Flurbiprofen with CYP2C9. An improved version of the Randles-Sevcik equation that accounts for drug interactions and a description of the effect of multiple drugs in the final current peak based on Gaussian analysis have been proposed.

In conclusion, the proposed sensors provide an innovative solution for point-of-care monitoring in the personalization of drug therapies, as well as in pharmacokinetic studies in both animals and humans. Since some pharmacokinetic studies are sequential, an optimal use of this technology can accelerate drug development by several months, saving great amounts of money.

Acknowledgements

Giuseppe Dino Albini is acknowledged for the Monte Carlo simulations. Victoria Shumyantseva is acknowledged for supporting in electrochemistry of P450 and for supplying the isoform 2B4. Federico Angiolini and Vasileios Pavlidis are acknowledged for helping with manuscript proof-reading. The research is financially supported by the SNF Sinergia Project CRSII2_127547/1 entitled "Innovative Enabling Micro-Nano-Bio-technologies for Implantable systems in molecular medicine and personalized therapy".

Appendix A. Supplementary data

Supplementary data associated with this article can be found, in the online version, at doi:10.1016/j.bios.2011.03.009.

References

Abramoff, M.D., Magelhaes, P.J., Ram, S.J., 2004. Biophotonics Int. 11, 36–42.
Aspinall, M., Hamermesh, R., 2007. Harv. Bus Rev. 85 (10), 108–117.
Bard, A.J., Faulkner, L.R., 2001. Electrochemical Methods–Fundamental and Applications, Second edition. John Wiley & Sons, New York, Equation (6.2.18) at page 231.
Boero, C., Carrara, S., De Micheli, G., 2009. Proceedings of IEEE/PRIME 2009 5th Conference on PhD Research in Microelectronics and Electronics , Ireland, Cork June 2009, pp. 72–75.
Carrara, C., Bavastrello, V., Ricci, D., Stura, E., Nicolini, C., 2005. Sens. Actuators B 109, 221–226.
Carrara, S., Shumyantseva, V., Archakov, A., Samorì, B., 2008. Biosens. Bioelectron. 24 (1), 148–150.
Carrara, S., Cavallini, A., Garg, A., De Micheli, G., 2009. Proceedings of the IEEE/ICME International Conference on Complex Medical Engineering , April 9–11, 2009, Tampe, Arizona, USA, pp. 1–6.
Daly, A., 2007. Curr. Opin. Drug Discov. 10 (1), 29–36.
De Leon, J., Susce, M., Murray-Carmichael, E., 2006. Mol. Diagn. Ther. 10 (3), 135–151.
Eichelbaum, M., Somogyi, A., Unruh, G., Dengler, H., 1981. Eur. J. Clin. Pharmacol. 19 (2), 133–137.
Frank, D., Jaehde, U., Fuhr, U., 2007. Eur J. Clin. Pharmacol. 63 (4), 321–333.
Hammersley, J.M., Handscomb, D.C., 1975. Monte Carlo Methods. Fletcher & Son Publisher, Norwich (UK), first edition in 1964, reprinted in 1975.
Iwuoha, E., Ngece, R., Klink, M., Baker, P., 2007. IET Nanobiotechnol. 1 (4), 62–67.
Johnson, D., Lewis, B., Elliot, D., Miners, J., Martin, L., 2005. Biochem. Pharmacol. 69 (10), 1533–1541.
Joseph, S., Rusling, J., Lvov, Y., Friedberg, T., Fuhr, U., 2003. Biochem. Pharmacol. 65 (11), 1817–1826.
Juma, F.D., Rogers, H.J., Trounce, J.R., 1979. Br J. Clin. Pharm. 8, 209–217.
Kashuba, A., Bertino, J., 2003. In: Piscitelli, S., Rodvold, K.A. (Eds.), Drug Interactions in Infectious Diseases. , 1st ed. Humana Press, Totowa, USA, pp. 13–39.

Kiselyova, O., Yaminsky, I., Ivanov, Y., Kanaeva, I., Kuznetsov, V., Archakov, A., 1999. Arch. Biochem. Biophys. 371 (1), 1–7.
Korzekwa, K.R., Krishnamachary, N., Shou, M., Ogai, A., Parise, R.A., Rettue, A.E., Gonzales, F.J., Tracy, T.S., 1998. Biochemistry 37, 4137–4147.
Lazarou, J., Pomeranz, B., Corey, P., 1998. Jama 279 (15), 1200.
Lin, J., 2007. Curr. Drug Metab. 8 (2), 109–136.
Liu, S., Peng, L., Yang, X., Wu, Y., He, L., 2008. Anal. Biochem. 375 (2), 209–216.
Locuson, C.W., Tracy, T.S., 2006. Drug Metab. Dispos, 34 (12), 1954–1957.
Mc Naught, A.D., Wilkinson, A., 1997. IUPAC. Compendium of Chemical Terminology 2nd ed. (the "Gold Book"). Blackwell Scientific Publications, Oxford.
Naka, T., Sakamoto, N., 1992. J. Membr. Sci. 74, 159–170.
Peng, L., Yang, X., Zhang, Q., Liu, S., 2008. Electroanalysis 20 (7), 803–807.
Schepers, R., Oyler, J., Joseph Jr., R., Cone, E., Moolchan, E., Huestis, M., 2003. Clin. Chem. 49 (1), 121.
Shumyantseva, V., Carrara, S., Bavastrello, V., Jason Riley, D., Bulko, T., Skryabin, K., Archakov, A., Nicolini, C., 2005. Biosens. Bioelectron. 21 (1), 217–222.
Shumyantseva, V.V., Bulko, T.V., Rudakov, Y.O., Kuznetsova, G.P., Samenkova, N.F., Lisitsa, A.V., Karuzina, I.I., Archakov, A.I., 2007. J. Inorg. Biochem. 101 (5), 859–865.
Struck, R., Alberts, D., Horne, K., Phillips, J., Peng, Y., Roe, D., 1987. Cancer Res. 47 (10), 2723–2726.
Tracy, T.S., 2003. Curr. Drug Metab. 4, 341–346.
Turner, S., Schwartz, G., Boerwinkle, E., 2007. Hypertension 50 (1), 1–5.
Yano, J.K., Wester, M.R., Schoch, G.A., Griffin, K.J., Stout, C.D., Johnson, E.F., 2004. J. Biol. Chem. 279, 38091–38094.